

Measurement of Magneto-Plasma Excitation Relaxation Time in the Two-Dimensional Electron System

I. V. Andreev,^{1, a)} V. M. Muravev,¹ V. N. Belyanin,^{1, 2} and I. V. Kukushkin¹

¹⁾*Institute of Solid State Physics RAS, Chernogolovka, 142432, Russia*

²⁾*Moscow Institute of Physics and Technology, Dolgoprudny, 141700, Russia*

(Dated: 30 September 2014)

Dependence of cyclotron magneto-plasma mode relaxation time on electron concentration and temperature in the two-dimensional electron system (2DES) in GaAs/AlGaAs quantum wells has been studied. Comparative analysis of cyclotron and transport relaxation time has been carried out. It was demonstrated that with the temperature increase transport relaxation time tends to cyclotron relaxation time. It was also shown that cyclotron relaxation time, as opposed to transport relaxation time, has a weak electron density dependence. The cyclotron time can exceed transport relaxation time by an order of magnitude in a low-density range.

In recent years plasma effects in two-dimensional electron systems (2DES) have been actively studied. Such interest is aroused by a number of unique properties distinguishing 2D plasmons from their 3D analogs. Plasma excitation parameters in 2DES are easily controllable by varying electron concentration in the system and applying an external magnetic field. Due to this fact 2D plasmon is a very flexible and convenient object for studying wave optics and light-matter interaction effects. As examples, plasmon interference observation¹, plasmonic Tamm states discovery² and implementation of ultra-strong light-2DES coupling in a plasmon polariton system in a microwave resonator³ could be mentioned. Scientific interest in the study of 2D plasma excitations is supported by potential applications in spectroscopy and detection of sub-terahertz radiation⁴.

One of the main restrictions to plasmon optics components creation is that the size of such devices should not substantially exceed the plasmon mean free path $L = v_p \tau$ (v_p - plasma excitation rate, τ - excitation relaxation time). It was the restriction, which constrained the studies in the field in the early days of studying 2D systems^{5, 6}. Achievements in molecular-beam epitaxy of the last two decades have resulted in creation of structures with electron mobility $\mu > 10^6$ cm²/V·s. In the structures like that plasmon free path may reach several millimeters, which enables to create plasmon optics components by conventional optical lithography technique⁷. It makes the problem of studying plasmon relaxation time and its dependence on various 2DES parameters highly relevant.

It is known that relaxation time has practically no dependence on magnetic field for magneto-plasma excitation, which in strong fields asymptotically approaches cyclotron resonance. To estimate the cyclotron resonance relaxation time, the full quantum lifetime $\tau_{CR} = \tau_q = [\int W_{pp'} dp']^{-1}$, is often used, which differs from the transport relaxation time $\tau_t = [\int W_{pp'} (1 - \cos \theta) dp']^{-1}$ in that it has no factor for low-angle scattering inefficiency (θ - scattering angle, $W_{pp'}$ - probability of scattering be-

tween the states with p and p' impulses). It is generally believed that $\tau_q/\tau_t \ll 1$ for the long-range scattering potential, and $\tau_q/\tau_t \approx 1$ for the short-range scattering one. The problem of the ratio between cyclotron resonance and transport relaxation times has been touched upon in a number of works, but has not been properly covered in theory and experiments so far⁸⁻¹⁰. Therefore, direct experimental study of this problem carried out within the framework of this paper is of considerable interest.

The experiments were carried out on GaAs/Al_{0.3}Ga_{0.7}As heterostructures with a 20 nm quantum well located at a 400 nm beneath the crystal surface. Three types of structures with different electron concentration were used. The 1st type of the structures has the electron concentration $n_s = 2.4 \times 10^{11}$ cm⁻². In the 2nd and the 3rd type of the structures the concentration was changed by optical depletion within $2 \times 10^9 \div 6.0 \times 10^{10}$ cm⁻² and $6 \times 10^{10} \div 3 \times 10^{11}$ cm⁻², respectively¹¹. The sample under consideration was a disk-shaped mesa with the $d = 1$ mm diameter produced by means of the optical lithography and wet etching. The disk was situated in the slot of a 50Ω microstrip line (Fig. 1(c)). The microwave radiation with the $f = 0.1 \div 40$ GHz frequency was guided to microstrip line via a matched coaxial cable. The microstrip line was used for resonance excitation of a plasma wave in the 2DES disk by electric field concentrated in the line slot. For plasma excitation detection two complementary techniques were used: measuring microwave transmission of a microstrip line¹² and optical detection of microwave absorption¹³. The sample was put into a helium cryostat with a superconducting magnet. Magnetic field was applied perpendicular to the sample surface. The measurements were carried out in the temperature range $T = 1.5 \div 100$ K.

Fig. 1(a) shows typical magnetic field dependencies of microstrip line microwave transmission measured for the structure with the electron concentration $n_s = 2.4 \times 10^{11}$ cm⁻² for the three temperatures of the sample: $T = 4.2, 21, 56$ K. The curves show resonance corresponding to microwave absorption when plasmon is being excited in the 2DES disk. Microwave transmission measurements were carried out using the lock-in tech-

^{a)}Electronic mail: andreev@issp.ac.ru

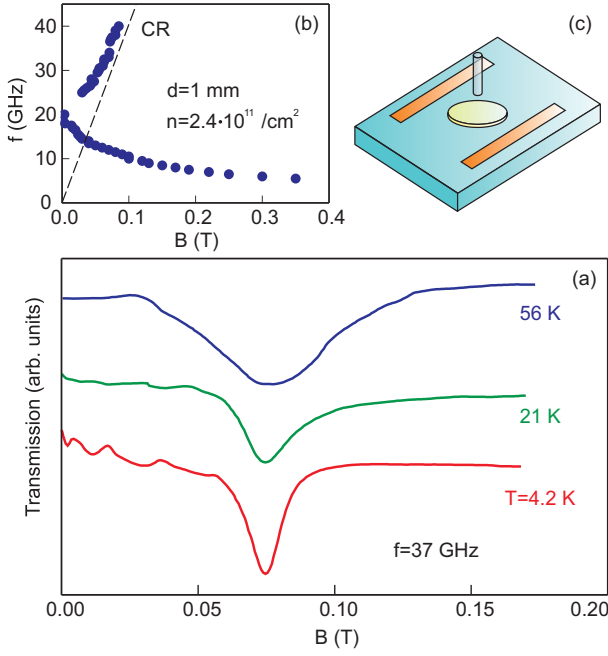


FIG. 1. (a) Magnetic field dependencies of microstrip line microwave transmission measured on 1 mm disk (structure 1) at the probe signal frequency $f = 37$ GHz for the temperatures $T = 56$ K, 21 K, 4.2 K. (b) Magnetic field dependence of magneto-plasma resonance obtained on the same structure. (c) Sample pattern. The mesa has the disk shape with the $d=1$ mm diameter. On each side of the mesa metal coating of the microstrip line to which microwave radiation was applied is observed. An optic fiber was fitted above the sample to detect plasma excitation using the optical technique.

nique. Generator output power was modulated with the 810 Hz frequency. The modulated microwave signal from the microstrip line output was transmitted to the Schottky detector input via the coaxial cable. The detector signal was measured by a lock-in amplifier. Fig. 1(b) shows resonance frequency dependence on magnetic field. The observed magneto-dispersion curve consists of two branches. The lower one corresponds to the edge magneto-plasma mode, which frequency lowers with magnetic field increase^{14,15}. The upper one corresponds to the cyclotron magneto-plasma mode asymptotically approaches cyclotron resonance in the limit of high magnetic fields. For the disk-shaped sample with the d diameter, the frequencies of the both magneto-plasma modes are described by the following expression¹⁴:

$$\omega_{\pm} = \pm \frac{\omega_{\text{CR}}}{2} + \sqrt{\omega_p^2 + \left(\frac{\omega_{\text{CR}}}{2}\right)^2}, \quad (1)$$

where $\omega_{\text{CR}} = eB/m^*$ - is cyclotron frequency (e - electron charge, B - magnetic field, $m^* = 0.067m_0$ - electron effective mass in GaAs), and ω_p - is the frequency of plasma oscillations in the disk in the zero magnetic field⁵:

$$\omega_p^2 = \frac{n_s e^2}{2m^* \epsilon \epsilon_0} q, \quad (2)$$

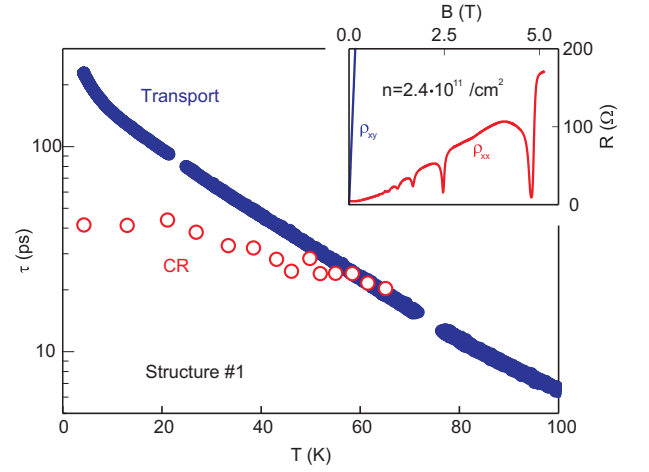


FIG. 2. Temperature dependencies of transport relaxation time (Transport) and relaxation time based on the cyclotron resonance width (CR). The measurements were carried out on structure 1. The inset shows magnetic field dependencies of resistivity tensor ρ components for the same structure measured by the transport technique in Hall bar geometry.

where ϵ is the average value of relative electrical permittivity of vacuum and GaAs, ϵ_0 is permittivity of free space, and $q = 2.4/d$ is plasmon wavevector in the disc. It is known that half-width of 2D electron cyclotron resonance is determined by the following relation^{8,16}:

$$\Delta\omega = \frac{1}{\tau_{\text{CR}}} + \Gamma. \quad (3)$$

Here τ_{CR} is electron scattering time during their cyclotron orbit motion, and Γ is cyclotron resonance radiative linewidth. For samples with the size $d \ll \lambda$ radiative linewidth can be evaluated as⁸

$$\Gamma = \Gamma_0 (d/\lambda)^2, \quad \Gamma_0 = \frac{n_s e^2}{2m^* c \epsilon_0}. \quad (4)$$

Here λ is the wavelength of electromagnetic radiation exciting the plasmon. In most part of previous experimental works^{9,10,17} due to the fact that $d \gg \lambda$ the cyclotron resonance width was almost fully determined by radiative decay rate Γ_0 . This fact made systematic measurements of the τ_{CR} and its dependence on 2DES parameters impossible.

In this experiment for disks with the $d = 1$ mm diameter and microwave frequencies up to 40 GHz the opposite limit $d \ll \lambda$ is realized, when $\Delta\omega$ is determined by the τ_{CR} only. For cyclotron resonance width measurement, the $f = 37$ GHz frequency was selected when the upper magneto-plasma mode approaching single-particle cyclotron resonance (Fig. 1(b)). Then $d\omega/dB = e/m^*$. This equation determines the ratio between the width of the cyclotron resonance $\Delta\omega$ measured by frequency sweep and its width ΔB measured by magnetic field sweep, and enables to convert one value into the other. The reasonability of this approach will be experimentally

proved in the second part of this letter. In the microwave transmission experiments magnetic field was swept at the $f = 37$ GHz fixed frequency (Fig. 1(a)). Then B -field cyclotron resonance linewidth was converted into the frequency linewidth, which was used to determine τ_{CR} from Eq. (3). The dependency of the τ_{CR} cyclotron relaxation time on the temperature T is marked on Fig. 2 in contour characters. It should be noted that we neglected the radiative broadening of the cyclotron resonance line, since for the sample used, according to (4) $\Gamma/2\pi \approx 0.3$ GHz, which is much less than the minimum resonance half-width in the experiments $\Delta f = 4$ GHz.

For reference, temperature dependency of transport relaxation time was calculated for the same structure

$$\tau_t = \frac{m^*}{n_s e^2 \rho_{xx}}.$$

Here ρ_{xx} is the diagonal resistivity tensor component in the zero magnetic field. Transport measurements were carried out in Hall bar geometry. This dependency is shown in the same figure by solid characters. The experimental data shows that temperature growth contributes to the decrease of the transport relaxation time, which approaches the cyclotron relaxation time. This result can be explained by the fact that at low temperatures electron scattering is mainly determined by the long-range donor potential, for which $\tau_q/\tau_t \ll 1$, and at high temperatures by electron-phonon scattering, for which, due to its isotropy, $\tau_q/\tau_t = 1$. Calculation of the quantum relaxation time from Shubnikov-de Haas oscillations attenuation results in $\tau_q \approx 1$ ps (inset to Fig. 2). It proves a significant effect of inhomogeneous broadening in the samples under consideration.

To study the dependency of cyclotron relaxation time on 2D electron concentration, the optical detection of microwave absorption was applied¹³. The spectra of 2D electron recombination luminescence measured under microwave irradiation and without it at the temperature 1.5 K were compared. For photoexcitation, a 780 nm wavelength stabilized semiconductor laser with about 0.1 mW output power was used. To guide the light from the laser to the sample and collect photoluminescence signal, the same optical fiber mounted directly above the mesa was used (Fig. 1(c)). The integral of absolute value of the difference of the spectra compared is a measure of microwave absorption intensity. The carrier density in 2DES was changed by optic depletion of the sample. Cyclotron resonance was measured using the optic technique for structures 2 and 3.

Typical dependencies of microwave absorption intensity on the frequency obtained by measurements for structure 2 in the magnetic field $B = 40$ mT for two electron densities are shown in Fig. 3(a). The figure clearly demonstrates a significant broadening of cyclotron resonance contour with the increase of electron density from $n_s = 0.32 \times 10^{10} \text{ cm}^{-2}$ to $1.31 \times 10^{10} \text{ cm}^{-2}$. Similar measurements carried out for a series of magnetic field values enable to restore magnetodispersion of the plasma

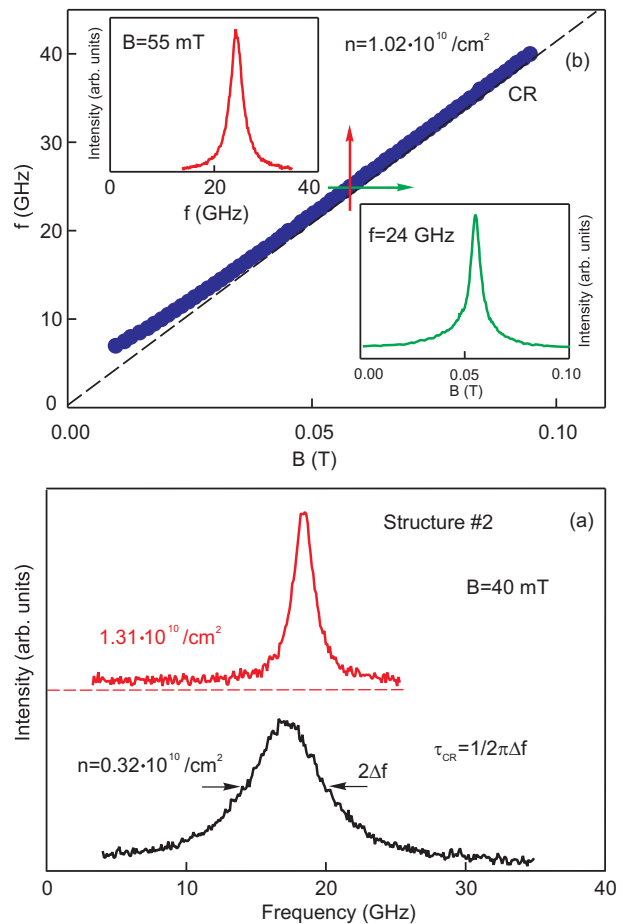


FIG. 3. (a) Dependencies of microwave absorption intensity on microwave frequency calculated for structure 2 using optical detection of microwave absorption for two electron densities. (b) Magnetic field dependency of microwave absorption resonance frequency calculated for the same structure. In the insets cyclotron resonance contours for the same magnetodispersion point calculated from frequency sweep (the upper inset) and magnetic field sweep (the lower inset).

mode under consideration (Fig. 3(b)). It is evident that the magneto-plasma mode observed in the experiments practically coincides with single-particle cyclotron resonance. The insets to Fig. 3(b) show resonance absorption dependencies on the microwave frequency measured at the constant magnetic field $B = 55$ mT by frequency sweep (top left) and at the constant microwave frequency $f = 24$ GHz by magnetic field sweep (bottom right). These two dependencies were measured for the same magnetodispersion curve point. It is evident that both the cyclotron magneto-plasma resonance detection techniques - by microwave frequency and magnetic field sweep - are in good agreement with each other, and $\Delta\omega$ and ΔB half-widths of resonance obtained using such techniques are indeed related to each other as magnetodispersion derivative $d\omega/dB = e/m^*$. It proves the procedures of calculation of the $\Delta\omega$ mode half-width from experimental data for ΔB applied in the first part of this letter.

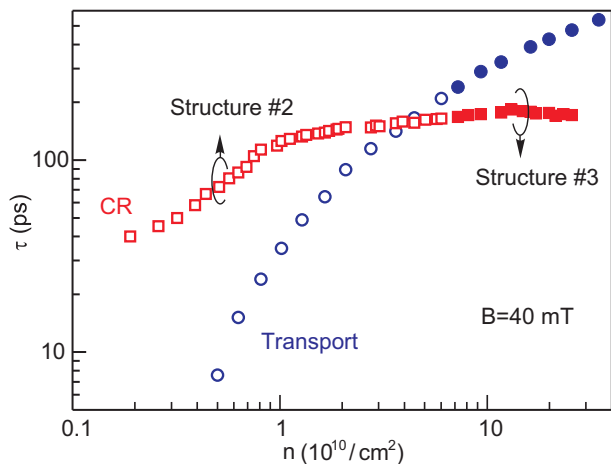


FIG. 4. Dependencies of transport relaxation time (circles) and cyclotron relaxation time (squares) on electron density. The contour characters correspond to structure 2, the solid characters to structure 3. The measurements were carried out by frequency sweep at the constant magnetic field $B = 40$ mT.

From Fig. 3(a) it follows that with the decrease of electron density the cyclotron resonance line significantly broadens. Thus, electron density is an important parameter affecting relaxation time in the system. Fig. 4 shows dependencies of cyclotron relaxation time measured by the optic technique and transport relaxation time on the density of 2D electrons in the sample for structures 2 and 3 overlapping the record wide range of electron densities ($2 \times 10^9 \div 3 \times 10^{11} \text{ cm}^{-2}$). It is evident that the transport scattering time depends heavily on the density changing by two orders of magnitude. On the other hand, the cyclotron scattering time much less depends on the density. In the $n_s > 4 \times 10^{10} \text{ cm}^{-2}$ electron density range the cyclotron time remains almost the same, and being apparently determined by low-angle electron scattering. It should be noted that plasmon free path changes insignificantly at such densities and amounts to $L = v_p \tau_{CR} \approx 2$ mm. In the low electron density region $n_s < 4 \times 10^{10} \text{ cm}^{-2}$ the τ_{CR}/τ_t ratio is greater than unity. For example, for the electron density $n_s = 10^{10} \text{ cm}^{-2}$ we have $\tau_t = 35$ ps, $\tau_{CR} = 105$ ps, so the cyclotron relaxation time exceeds the transport time three times. The exceedance of the cyclotron relaxation time over the transport time cannot be explained within the framework of a simple model, where $\tau_{CR} \simeq \tau_q$, since inefficiency of low-angle scattering should always result in the $\tau_q/\tau_t < 1$. inequation. Such transport scattering time behavior is apparently due to carrier localization at low densities. In this case the transport technique allows to measure carrier relaxation time only for delocalized states having the millimeter spatial scale compatible with the sample size. On the other hand, the cyclotron relaxation time is determined by scattering of electron states having the micron spatial scale determined by the cyclotron orbit radius. This result qualitatively corresponds to the results ob-

tained for high-mobility Si/SiGe heterostructures in the work⁹.

In this letter we studied the behavior of cyclotron relaxation time in 2DES using two cyclotron resonance detection techniques: based on the signal absorption in a microstrip line and based on the change of the photoluminescent spectrum. It has been shown that the transport relaxation time tends to the cyclotron relaxation time with the temperature increase. Both the transport and the cyclotron relaxation times coincide at temperatures $T > 60$ K. It has been demonstrated that the cyclotron relaxation time, as opposed to the transport time, has a weak dependence on the electron density. This fact can not be explained within the framework of existing theories.

The work was carried out under financial support of the Russian Scientific Foundation, grant no. 14-12-00599.

- ¹I. V. Kukushkin, M. Y. Akimov, J. H. Smet, S. A. Mikhailov, K. von Klitzing, I. L. Aleiner, and V. I. Falko, *Phys. Rev. Lett.* **92**, 236803 (2004); V. M. Muravev, A. A. Fortunatov, I. V. Kukushkin, J. H. Smet, W. Dietsche, and K. von Klitzing, *ibid.* **101**, 216801 (2008).
- ²G. C. Dyer, G. R. Aizin, S. J. Allen, A. D. Grine, D. Bethke, J. L. Reno, and E. A. Shaner, *Nature Photonics* **7**, 932 (2013).
- ³V. M. Muravev, I. V. Andreev, I. V. Kukushkin, S. Schmult, and W. Dietsche, *Phys. Rev. B* **83**, 075309 (2011); G. Scalari, C. Maissen, D. Turcinkova, D. Hagenmuller, S. De Liberato, C. Ciuti, C. Reichl, D. Schuh, W. Wegscheider, M. Beck, and J. Faist, *Science* **335**, 1323 (2012).
- ⁴I. V. Kukushkin, S. A. Mikhailov, J. H. Smet, and K. von Klitzing, *Appl. Phys. Lett.* **86**, 044101 (2005); W. Knap, M. Dyakonov, D. Coquillat, F. Teppe, N. Dyakonova, J. Lusakowski, K. Karpierz, M. Sakowicz, G. Valusis, D. Seluta, I. Kasalynas, A. El Fatimy, Y. Meziani, and T. Otsuji, *J. Infrared Millim. Terahz Waves* **30**, 1319 (2009); V. Popov, *ibid.* **32**, 1178 (2011); V. M. Muravev and I. V. Kukushkin, *Appl. Phys. Lett.* **100**, 082102 (2012).
- ⁵F. Stern, *Phys. Rev. Lett.* **18**, 546 (1967).
- ⁶S. J. Allen, D. C. Tsui, and R. A. Logan, *Phys. Rev. Lett.* **38**, 980 (1977).
- ⁷V. M. Muravev, I. V. Kukushkin, A. L. Parakhonskiy, J. Smet, and K. von Klitzing, *JETP Letters* **83**, 246 (2006); V. M. Muravev, I. V. Andreev, I. V. Kukushkin, J. H. Smet, and K. von Klitzing, *ibid.* **87**, 577 (2008).
- ⁸S. A. Mikhailov, *Phys. Rev. B* **54**, 10335 (1996).
- ⁹R. Masutomi, K. Sasaki, I. Yasuda, A. Sekine, K. Sawano, Y. Shiraki, and T. Okamoto, *Phys. Rev. Lett.* **106**, 196404 (2011).
- ¹⁰Q. Zhang, T. Arikawa, E. Kato, J. L. Reno, W. Pan, J. D. Watson, M. J. Manfra, M. A. Zudov, M. Tokman, M. Erukhimova, A. Belyanin, and J. Kono, *Phys. Rev. Lett.* **113**, 047601 (2014).
- ¹¹I. V. Kukushkin, K. von Klitzing, K. Ploog, V. E. Kirpichev, and B. N. Shepel, *Phys. Rev. B* **40**, 4179 (1989).
- ¹²L. W. Engel, D. Shahar, C. Kurdak, and D. C. Tsui, *Phys. Rev. Lett.* **71**, 2638 (1993); I. V. Andreev, V. M. Muravev, D. V. Smetnev, and I. V. Kukushkin, *Phys. Rev. B* **86**, 125315 (2012).
- ¹³B. M. Ashkinadze, A. Nazimov, E. Cohen, A. Ron, and L. N. Pfeiffer, *Phys. Status Solidi (a)* **164**, 523 (1997); M. Akimov, I. Kukushkin, S. Gubarev, S. Tovstonog, J. Smet, K. von Klitzing, and W. Wegscheider, *JETP Letters* **72**, 460 (2000).
- ¹⁴S. J. Allen, H. L. Störmer, and J. C. M. Hwang, *Phys. Rev. B* **28**, 4875 (1983).
- ¹⁵V. Volkov and S. Mikhailov, *Sov. Phys. JETP* **67**, 1639 (1988).
- ¹⁶K. Chiu, T. Lee, and J. Quinn, *Surf. Sci.* **58**, 182 (1976).
- ¹⁷G. Abstreiter, J. P. Kotthaus, J. F. Koch, and G. Dorda, *Phys. Rev. B* **14**, 2480 (1976).